

Time-domain Classification of the Brain Reward System: Analysis of Natural- and Drug-Reward Driven Local Field Potential Signals in Hippocampus and Nucleus Accumbens

AmirAli Kalbasi^{a,1}, Shole Jamali^{b,1}, Mahdi Aliyari Shoorehdeli^{a,*}, Alireza Behzadnia^c, Abbas Haghparast^b

^a*Department of Mechatronics, Faculty of Electrical Engineering, K. N. Toosi University of Technology, Tehran, Iran*

^b*Neuroscience Research Center, School of Medicine, Shahid Beheshti University of Medical Sciences, Tehran, Iran*

^c*Histopathology Department, Leeds Teaching Hospital NHS Trust, Beckett Street, Leeds, West Yorkshire, LS9 7TF*

¹*The first two authors contributed equally to this work*

Abstract

Addiction is a major public health concern characterized by compulsive reward-seeking behavior. The excitatory glutamatergic signals from the hippocampus (HIP) to the Nucleus accumbens (NAc) mediate learned behavior in addiction. Limited comparative studies have investigated the neural pathways activated by natural and unnatural reward sources. This study has evaluated neural activities in HIP and NAc associated with food (natural) and morphine (drug) reward sources using local field potential (LFP). We developed novel approaches to classify LFP signals into the source of reward and recorded regions by considering the time-domain feature of these signals. Proposed methods included a validation step of the LFP signals using autocorrelation, Lyapunov exponent and Hurst exponent to assess the meaningful stability of these signals (lack of chaos). By utilizing the probability density function (PDF) of LFP signals and applying Kullback-Leibler divergence (KLD), data were classified to the source of the reward. Also, HIP and NAc regions were visually separated and classified using the symmetrized dot pattern technique, which can be applied in real-time to ensure the deep brain region of interest is being targeted accurately during LFP recording. We believe our method provides a computationally light and fast, real-time signal analysis approach with real-world implementation.

Keywords: Time-domain classification, Probability density function, Kullback-Leibler divergence, symmetrized dot pattern, Correlation, Drug-reward, Natural-reward, Local field potential, Hippocampus, Nucleus accumbens

1. Introduction

Addiction is a major public health concern characterized by frequent and compulsive reward-seeking behavior, often in the form of natural or unnatural substance abuse but can also include other stimuli such as hypersexuality or gambling. When considering natural and unnatural sources of reward, although some studies have suggested behavioral and neurochemical differences between the two, limited studies have compared the neural pathways activated via drugs and naturally induced types of rewards [23, 24, 32, 45].

The mesolimbic pathway is responsible for the reward system, with the ventral striatum (VS) and ventral tegmental area (VTA) being the most important. The effector neural projections from the VTA to the nucleus accumbens (NAc) are associated with motivation and reward whilst the excitatory glutamatergic signals from the hippocampus (HIP) to NAc mediate learned behavior in addiction. Hippocampal activity is also important in reward acquisition and expression phases [1, 36, 42].

In order to investigate the functional connectivity of NAc and HIP as two crucial areas of a reward system in drug vs. natural sources of reward, a conditioned place preference paradigm (CPP) was designed [7] using morphine and food to study the drug vs. naturally induced local field potentials (LFP) in NAc and HIP simultaneously, in male Wistar rats' brain, by considering a novel approach in analyzing the time-domain feature of the LFP signals [22, 37].

Different signal processing methods exist to analyze and interpret neural circuit activities. Whilst choosing the method is the most critical step in analyzing the experimental results, no standard approach has been reported [4, 44]. Therefore, choosing an appropriate method is an important challenge that neuroscientists should be acutely aware of when interpreting signaling data.

In general, certain supervised or unsupervised statistical learning methods, like machine learning, are less desirable

for understanding specific features. Accessing specific weights and biases of signal features in non-transparent black-box classification techniques is not readily permissible. Thus, features that may be surrogates of underlying biological mechanisms are lost in the analyses [9, 38]. When considering non-machine learning approaches, statistical signal processing methods extract signal features using time, frequency, or time-frequency domains [2, 5, 39].

Studies of neural circuits in the literature often focus on frequency or time-frequency domains of signals, with only a few employing time-domain signal analysis. The time-domain analysis examines the basic features of the signal rather than the computationally intensive methods using frequency and time-frequency domains [14, 47]. It allows for more interpretable results and less computational complexity for analyzing in real-time implementation.

Among the limited studies on time-domain feature extraction in signal analysis, often basic time features such as mean, harmonic mean, mean absolute deviation, range and inter-quartile range, variance, covariance, and power, as well as entropy, moment, skewness, Kurtosis, percentile, and Gradient, had been used. Previous studies have utilized the above features to classify EEG signals as macroscale signals of cortical activity to detect epileptic seizures [11, 13].

This study adopted a new approach to classify LFP signals by extracting time-domain features. Time-domain data were preprocessed and then validated using methods in detecting chaos: the Hurst and Lyapunov exponent. Kullback-Leibler divergence (KLD) was used to separate morphine and food-driven signal pathways based on the difference in the probability density functions (PDF) of reward signals in the HIP, NAc (one-dimensional PDFs), and HIP-NAc (two-dimensional PDF). Also, the symmetrized dot pattern (SDP) method was used to visually separate HIP and NAc signals.

To the best of our knowledge, no previous study has attempted to classify LFP time-domain signals as mesoscale signals of deep and focal brain areas using KLD and SDP methods. Additionally, we attempt to preprocess neural circuit using a chaotic or non-chaotic approach.

The proposed approach successfully classified LFP signals into a source of reward (morphine vs. food vs. saline) and the source of signal from the brain area (HIP vs. NAc). We believe our method provides a computationally light and fast, real-time signal analysis approach that can be implemented in laboratory and clinical settings to provide meaningful insight into deep brain activities when investigating neurobehavioral conditions such as addiction.

The content of this paper was structured as follows. The behavioral and electrophysiological tests were presented in Section II. Section III explained the data hierarchy and data preprocessing and validation. Section IV described the time-domain classification methods and results, and Section V summarized the research and concluded the study.

2. Behavioral and electrophysiological tests

2.1. Animals and Surgery

Male Wistar rats (Pasteur Institute, Tehran, Iran; weighing 220–270 g) were housed under standard laboratory conditions (12/12h light/dark cycle in temperature ($25\pm 2^\circ\text{C}$) and humidity ($55\pm 10\%$)). Animals were restricted for food until they were reduced to 80–85% of their free-feeding body weight before the conditioning phase. The Ethics Committee approved all protocols of Shahid Beheshti University of Medical Sciences, Tehran, Iran (IR.SBMU.SM.REC.1395.373) and followed the National Institutes of Health Guide for the Care and Use of Laboratory Animals (NIH Publication; 8th edition, revised 2011). The rats were anesthetized using a cocktail of Ketamine and Xylazine (100/10 mg/kg; intraperitoneal (IP)) and placed stereotaxic apparatus (SR-8N, Narishige, Japan); the skin was incised, the skull was cleaned, and a hole was opened above of each target areas hippocampal CA1 (anteroposterior: -3.4 mm, lateral: ± 2.5 mm); NAc (anteroposterior: +1.5 mm, lateral: ± 1.5 mm). The recording electrodes were implanted into HIP (dorso-lateral: -2.6 mm) and NAc (dorso-lateral: -7.6 mm) to simultaneously record local field potentials (LFPs) in these areas. The reference and ground screws were inserted in the skull (Fig. 1.A.a-d). The rats were allowed to recover for ten days following surgery [27, 30].

2.2. Drugs and Food

Ketamine and Xylazine were obtained from Alfasan Chemical Co, Woerden, Holland. Morphine sulfate (Temad, Iran) was dissolved in physiological saline (0.9% NaCl) and administered by a subcutaneous (s.c.) route at the dose of 5mg/kg for morphine (drug) conditioning and 6g of Hobby© biscuits for food conditioning.

2.3. Conditioned place preference paradigm

The conditioned place preference paradigm (CPP) apparatus consisted of three-chamber polyvinyl chloride boxes; two large side chambers (equal size) were connected to a smaller one (Null; with a smooth PVC floor). The two larger chambers differed in their floor texture (smooth or rough) and wall stripes pattern (horizontal or vertical) that provided distinct contexts that were paired with morphine, food, or vehicle (saline injections). Guillotine doors separated three distinct chambers. The CPP procedure consists

of three phases: 1) pre-conditioning, 2) conditioning, and 3) post-conditioning.

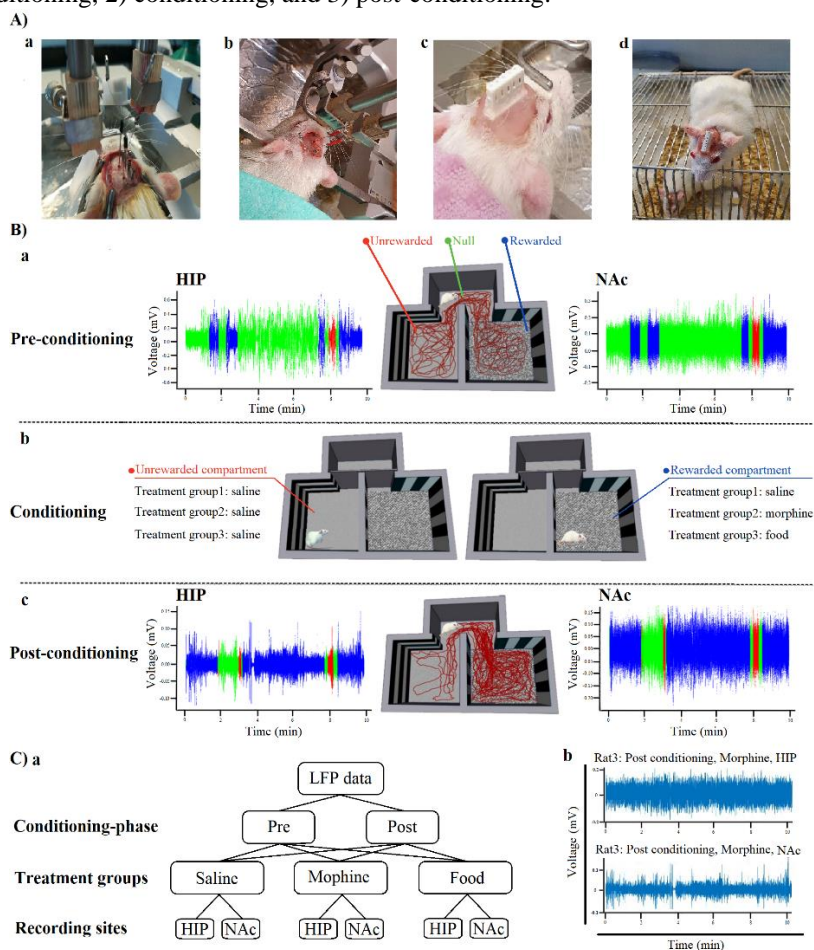


Fig. 1. Behavioral and LFP recording protocol. **A.a-d)** Electrode's implementation surgery; **B)** Conditioning phases: **B.a)** Pre-conditioning, A recorded sample from the HIP (left panel), Schematic of freely moving rat (middle-panel), A recorded sample from NAc (right panel); **B.b)** Schematic of conditioning; **B.c)** Post-conditioning: Recorded sample from the HIP (left panel), Schematic of freely moving rat (middle panel), A recorded sample from NAc (right panel); **C.a)** Labeling structure; **C.b)** Example of labeled data in Rat3.

During the pre-and post-conditioning phases, rats freely explored the entire arena for 10 minutes while they were connected to the LFP recording cable.

1) Pre-conditioning phase

Twenty-four hours before the conditioning phase, each animal was given free access to all three compartments. The animal was placed in the CPP apparatus for 10min. The time spent in each compartment was recorded and measured using a 3CCD camera. Animals that showed an inherent preference, defined as spending more than 80% of the time in one compartment during CPP, were excluded from the experiment (Fig. 1.B.a).

2) Conditioning phase (Saline, Morphine, Food)

For morphine conditioning, each animal received a subcutaneous (s.c.) injection of morphine (5 mg/kg) as a drug reward and was placed and restricted (the sliding door was kept closed) in the reward-paired compartment (rewarded) of the CPP apparatus for 30min. For food conditioning, animals received food pellets (6g of Hobby biscuits) in the middle of the reward-paired compartment (rewarded) for 30min. Following six h, each animal in the drug- or food-CPP group experienced an injection of saline (1 ml/kg; s.c) as the vehicle of morphine, or nothing, respectively, in the non-reward compartment (unrewarded) for 30min. On the following day, the previous day, the morning protocol was switched to the afternoon and vice versa throughout the experiment. The mentioned protocol was conducted to the end of the conditioning phase (three days for the morphine CPP and five days for the food CPP) (Fig. 1.B.b) [17, 18].

3) Post-conditioning phase

Twenty-four hours after the conditioning phase, each animal was tested under a food- or morphine-free condition with free access to all three compartments. The animal was placed in the CPP apparatus for 10min. The time spent in each

compartment was recorded and measured using a 3CCD camera. The conditioning score (CPP score) was calculated by subtracting the time spent in the unrewarded paired compartments from the rewarded paired compartment (Fig. 1.B.c).

2.4. Behavioral and LFP recording

LFP recordings were collected from hippocampal CA1 and NAc of freely moving rats during pre-and post-conditioning while the animal performed the CPP procedure. The animal's behavior was recorded with a digital video camera (30 frames per second), and movements were tracked by an automated system synchronized with behavioral data and electrophysiological recordings. The spatial position was defined as the animal's head in each frame. A lightweight and flexible cable was connected to the pins on the head-stage preamplifier. Recordings, digitalization, and filtering of neural activities were performed using a commercial acquisition processor (NikteK, IR). LFP recordings were sampled at 1000 Hz. Fig. 1.C.b shows a sample of recorded LFP from HIP (top) and NAc (bottom) for 10-min in the rat that had received morphine.

At the end of the experiments, the electrode trace was marked with the electrical lesion (25 μ A, 10s) before the animals were perfused with isotonic saline followed by 10% formalin. Brains were sliced (150 μ m) using a vibrating microtome (Campden Instruments, Germany). Electrode tip traces were localized using a light microscope and were confirmed using a rat brain atlas (Paxinos and Watson 2007).

3. Methodology

3.1. Data hierarchy

Data hierarchy was set based on three aspects of the CPP experiment, namely the phase of the experiment, treatment received during the CPP conditioning period (morphine vs. food vs. saline), and the site-specific LFPs (Fig. 1.C.a):

1. *Conditioning-phase*: pre-and post-conditioning phases correspond to the timing of LFP measurement before or after rats were conditioned to their treatment.
2. *Treatment groups*: animals received three different treatments during the conditioning phase: morphine, food, or saline.
3. *Recording sites*: local field potential signals recorded via implanted electrodes in either HIP or NAc.

3.2. Data Analysis

Data were analyzed by considering signals from either HIP or NAc separately (henceforth referred to as HIP/NAc) and the HIP and NAc connectivity (HIP-NAc) in the time domain in three steps: 1) *preprocessing*: noise and outlier reduction; 2) *validation*: evaluating meaningfulness of the captured signals, and 3) *feature extractions and signal classification*. All analyses were performed using MATLAB 2020b (The MathWorks, Inc., US) and Python (v3.7).

3.3. LFP signal preprocessing

Following schema integration of the databases and subsequent deduplication, relevant LFP signals were filtered to capture signals within the range of 0.5 to 300 Hz, truncating background activity (noise) to ensure accurate local neural activity recording. The conventional three-sigma limits were applied [40] to identify outliers and saturated data points and replaced these with arithmetic mean values.

3.4. LFP signal validation

LFP recordings of neuronal activity within an area of interest may become contaminated by the activity of neurons outside the area of interest. The recordings can also get corrupted due to faulty hardware, resulting in disjointed signals. To measure data quality, the Hurst exponent (H) of data and also autocorrelation of the LFP data were calculated to examine whether the recordings demonstrate long-term dependence (i.e., reflective of the sequential structure of neural activities associated with specific behavior) [8, 12, 21]. Next, the Lyapunov exponent (LE) was used to indicate chaotic signals (i.e., reflective of temporal dependency of neural activities on the initial excitatory or inhibitory signaling) [31].

Hurst exponent is a measure of the long-term dependence and randomness of the time-series data [12]. Equation (1) shows the Hurst exponent equation where; $R(n)$ is the range of the first n cumulative deviations from the mean, and $S(n)$ is their standard deviation $\mathbb{E}[x]$ is the expected value, $-n$ is the period of the observation, C is a constant.

H value of 0.5 indicates a lack of time-dependent correlation [3], whilst values higher or lower than 0.5 indicate a positive or negative of values at t_n in the series to the lagged values at t_{n-1} , respectively. In other words, the value of each data point (e.g., neural

activity at t_1) is dependent on the preceding values in the series (e.g., neural activity at t_0) and not based on pure chance [16, 34].

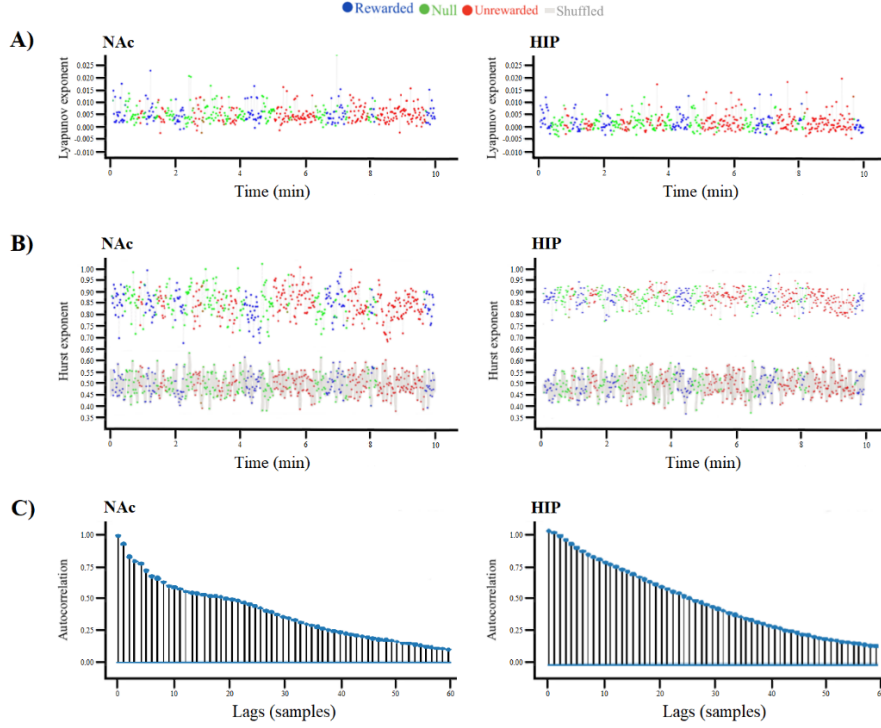


Fig. 2. Validation tests. A) Lyapunov exponent B) Hurst exponent C) Autocorrelation

The Lyapunov exponent was calculated for all LFP signals originating from either HIP or NAc during pre-conditioning and post-conditioning phases regardless of their treatment group (Fig 2.A). The global Lyapunov exponent of all rats shows a positive rate, close to zero. This can be interpreted as a weakly chaotic behavior capable of short-term predictions [48].

$$\mathbb{E} \left[\frac{R(n)}{S(n)} \right] = Cn^H \quad (1)$$

Autocorrelation (2) is the correlation of a signal with its delayed self [29]. As such, randomly generated signals (white noise) with no correlation between signals, the correlation between signals at $t = 1$ to signals at $t \neq 1$ is zero [10].

$$R_{XX}(t_1, t_2) = E[X_{t_1} \bar{X}_{t_2}] \quad (2)$$

Hurst exponent of the recorded LFP signals was significantly higher ($H \approx 1$) when compared to randomly generated data using shuffled LFP signals ($H \approx 0.5$), in 5s windows, with no overlaps (Fig 2.B). Additionally, the recorded LFP signals' autocorrelation was non-zero (≈ 0.95 in the first lag) (Fig 2.C). Therefore, the recorded LFP signals are meaningful, which indicates a predominant excitatory sequential neural signaling pattern. ($H > 0.5$).

Lyapunov exponent (λ) (3) is an indicator of the direction of time-series data, with large maximal Lyapunov exponents characteristic of irregular and non-periodic chaotic signals (similar to white-noise or impact noise) [6, 20].

$$|\delta Z(t)| \approx e^{\lambda t} |\delta Z_0| \quad (3)$$

where vector δZ diverges, and λ is the maximal Lyapunov exponent with initial separation vector δZ_0 (4) [46]:

$$\lambda = \lim_{t \rightarrow \infty} \lim_{|\delta Z_0| \rightarrow 0} \frac{1}{t} \ln \frac{|\delta Z(t)|}{|\delta Z_0|} \quad (4)$$

3.5. Hypothesis-test for validation of classification methods

Hypothesis testing was used to determine the significant difference between groups classified based on the methods that were used. Statistical hypothesis testing using conventional methods was performed after assessing assumptions ($\alpha = 0.05$). Normality was assessed using Kolmogorov-Smirnov test. Non-parametric Wilcoxon rank test and Mann-Whitney U tests were

used to determine the significance of inter-and and intra-group differences. Parametric paired and unpaired t-tests were used for two-group testing, and one-way analysis of variance (ANOVA) test with a post-*hoc* Tukey test was used for multi-group testing.

4. Time-domain-based features classification

4.1. Basic features

The initial analysis consisted of separating and classifying LFP signals into three groups (morphine, food, or saline); two phases (pre-and post-conditioning); and two recording sites (HIP and NAc) using basic and common characteristics such as mean, maximum, minimum, median, and standard deviation. However, the LFP signals did not appear to be significantly separated into the desired categories; therefore, other features of the signals were considered.

4.2. HIP-NAc correlation

The LFP signals were classified by considering the functional connectivity between the HIP and NAc regions. The Pearson correlation of HIP-NAc signals shows a strong significant correlation between these two regions in post-conditioned subjects being treated with food, while the other treatment groups did not show a significant or meaningful correlation ($-0.1 < r < 0.1$) (Fig 3). No correlation was found among the three treatment groups in the pre-conditioning phase.

These results indicate that the functional connectivity between HIP-NAc was increased following food treatment as a natural reward while it did not change following morphine reward; therefore, HIP-NAc functional connectivity is required for inducing food reward but not for the morphine reward induction.

4.3. One-dimensional probability distribution function

The correlation analysis highlighted the functional connectivity between HIP and NAc; however, neuroscientists are interested in studying the signal changes in each specific site separately. Given the LFP signals are continuous variables, the one-dimensional probability density function (1D-PDF) can be assumed to classify HIP and NAc according to the type of reward received based on the Bayes theorem. Uncovering the underlying PDF of data also enables us to have a more comprehensive description of the signal.

The maximum likelihood estimation method (MLE) estimated the most probable underlying density function [28] by considering multiple distributions. Results show that the Gaussian distribution was the most probable PDF of the LFP signals. The PDF of a Gaussian distribution ($f(x)$) is defined using two parameters, the mean (μ) and variance (σ) (5) [33].

$$f(x) = \frac{1}{\sigma\sqrt{2\pi}} e^{-\frac{1}{2}\left(\frac{x-\mu}{\sigma}\right)^2} \quad (5)$$

The Gaussian PDF estimated parameters of LFP signals from HIP (Fig. 4.A; left panel) and NAc (Fig. 4.A; right panel) regions were compared between pre-and post-conditioning phases in each saline, morphine, and food treatment groups (Fig. 4.A).

The results showed a significant difference in the PDF variance of the LFP signals in the NAc region of the subject treated with morphine (Fig. 4.A middle-right panel); with a reduced and narrower variance and amplitude of LFP signaling in post-conditioning compared to pre-conditioning. This reduction in the signaling amplitude has also been reported previously, where a reduced NAc signaling was observed following chronic morphine treatment [26]. There was no difference in NAc activity of the other two treatment groups between pre- and post-conditioning (Fig. 4.A top- and bottom-right panels).

Interestingly, the reverse in the HIP region in subjects treated with food (Fig. 4.A bottom-left panel), a variance of the HIP PDF after food-CPP was increased. No significant difference was seen in other groups (Fig. 4.A top- and middle-left panels).

According to these results, the conditioning phases could be separated based on the changes in the PDF parameters. Additionally, treatment groups could be separated. This was followed by Kullback–Leibler divergence to examine the difference between the PDFs of LFP signal more precisely.

The KLD was used to measure the similarity of LFP signals PDFs in pre-and post-conditioning phases of each treatment group in both HIP and NAc. The Kullback–Leibler divergence score is widely used to measure the similarity and relative entropy between two distributions [19].

The KLD aims to measure the information gained between two PDFs. For two probability distributions (P and Q) in the same domain C, the KLD of P from Q is defined as (6) [25].

$$KLD(P \parallel Q) = \sum_{c \in C} p(c) \log_2 \frac{p(c)}{q(c)} \quad (6)$$

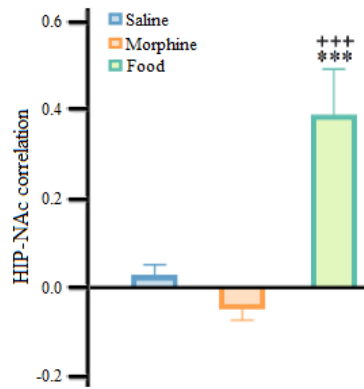


Fig. 3. HIP-NAc correlation. *** $P < 0.001$ compared with the saline and morphine groups in the post-conditioning phase.

The divergence is not symmetric. Thus $KLD(P \parallel Q) \neq KLD(Q \parallel P)$, with a non-negative possible value ($0 \leq KLD < +\infty$). The KLD is 0 if the two distributions are equal in their outcomes, namely $P(c) = Q(c), \forall c \in C$. It has no upper-bound, as shown by Gibbs' inequality [8]. Jensen-Shannon divergence (JSD) is used to solve this problem. The JS divergence is defined as (7) [35].

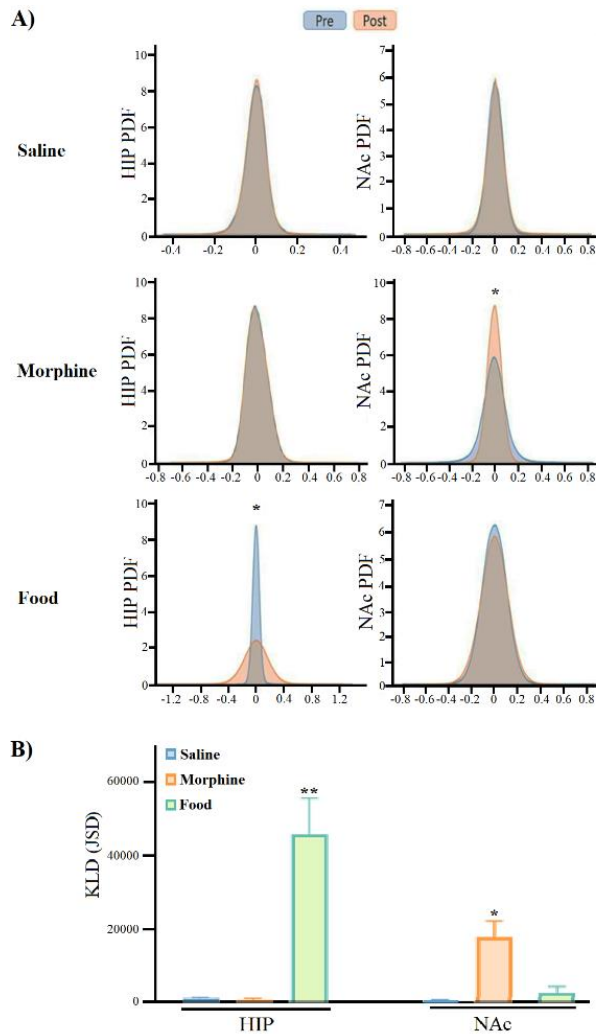


Fig. 4. One-dimensional probability density function of HIP/NAc. **A)** 1D-PDF of LFP recording data, * $P < 0.05$ as a comparison between pre-and post-conditioning phases in each treatment's groups (saline, morphine, and food); **B)** Comparing the KLD (JSD) of 1D PDF of LFP signals among saline, morphine, and food groups, ** $P < 0.01$ as a comparison of food group with saline and morphine groups in HIP; * $P < 0.05$ as comparison of morphine group with saline and food groups in NAc.

$$JSD(P, Q) = \frac{KL(P\|A) + KL(Q\|A)}{2} \quad (7)$$

For measuring KLD (JSD test), custom code was used in python 3.7.

To classify treatment groups into saline, morphine and food, the PDF similarity of pre-and post-conditioning phases were computed by JS-test. The higher calculated KLD (JSD) indicates a more significant difference between PDFs (or less similarity).

Figure 4.B left panel shows that KLD (JSD) of the HIP was significantly higher in the food-CPP group compared to saline (One-way ANOVA test with post-hoc Tukey test, $P < 0.01$) and morphine treatment groups (One-way ANOVA test with post-hoc Tukey test, $P < 0.01$); there was no significant difference between KLD of saline and morphine groups. Figure 4.B right panel shows that the KLD of NAc in the morphine group was more than both saline (One-way ANOVA test with post-hoc Tukey test, $P < 0.05$) and food (One-way ANOVA test with post-hoc Tukey test, $P < 0.05$) treatment groups, while there was no difference between the KLD of NAc between saline and food group. These results show that we can classify the LFP signals based on the calculated KLD for each recording site (HIP and NAc) into either food or morphine-CPP.

To follow the goal of classifying each animal's recorded LFP signals into their respective treatment group, a threshold was calculated for the KLD score based on the LFP recording of the saline group (control group) as the baseline. Setting the HIP KLD threshold as >1000 (KLD threshold in the HIP for the saline group; $HIP-KLD_{T.saline}$), subjects treated with food were successfully classified as the food treatment group (accuracy = 100%), and NAc KLD threshold as >900 (KLD threshold in the NAc for the saline group; $NAc-KLD_{T.saline}$) classified the subject correctly as the morphine treatment group (accuracy = 100%). If the calculated HIP KLD was less than 1000 and NAc KLD was less than 900, subjects were classified as saline (accuracy = 100%).

These results suggest that, as expected, there is no change in HIP and NAc LFP signals when subjects were not conditioned in response to saline-CPP. HIP activity in animals that were conditioned with food and NAc in those conditioned with morphine has essentially changed their signaling patterns. Therefore, HIP activity plays an essential role in food-induced reward (natural reward) while NAc activity is necessary for morphine-induced reward (drug reward).

4.4. Two-dimension multivariate probability distribution function (2D multivariate -PDF)

A two-dimension multivariate probability density function of the connectivity of HIP and NAc (HIP-NAc 2D-PDF) was estimated to classify the different treatment groups. The most likely distribution for two-dimensional PDFs was identified using the previously described maximum likelihood estimation method (MLE). Gaussian 2D-PDF proved to be the best fit. x is an $n \times 1$ random vector. The density function for a multivariate Gaussian distribution ($p(x)$) with mean μ and covariance matrix Σ is [43]:

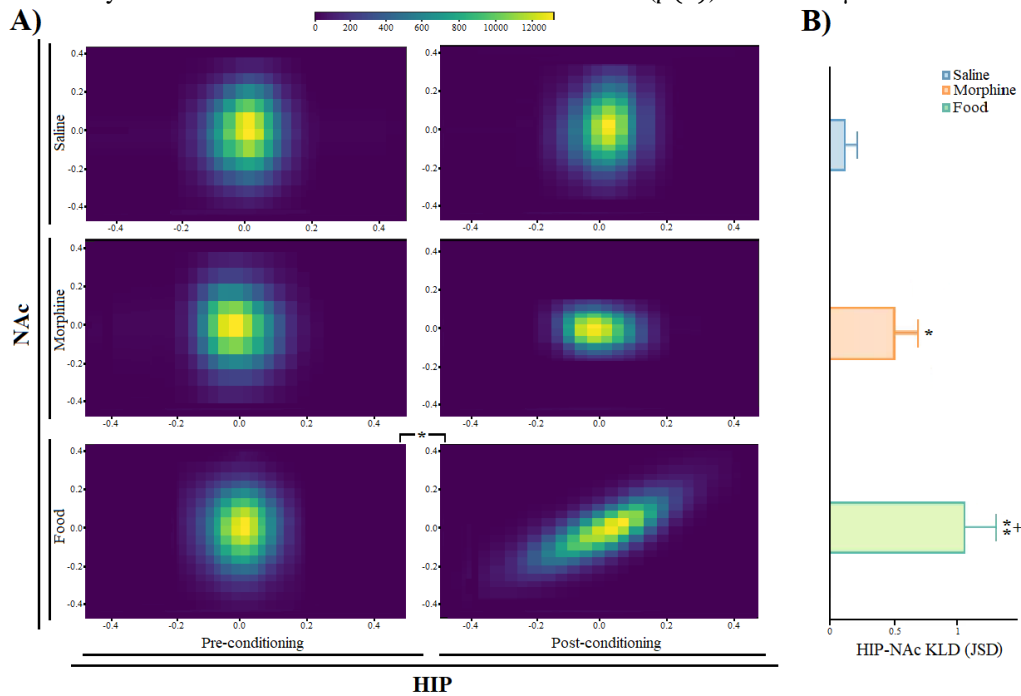


Fig. 5. HIP-NAc two-dimensional probability density function. A) 2D HIP-NAc PDF, $*P < 0.05$ as a comparison between pre- and post-conditioning phases in each treatment group (saline, morphine, and food); **B)** KLD (JSD) of 2D HIP-NAc PDF, $*P < 0.05$ as a comparison between saline and morphine groups, $**P < 0.01$ as a comparison between saline and food groups, $+P < 0.05$ as a comparison between morphine and food groups.

$$p(x) = \frac{1}{(2\pi)^{n/2} \det(\Sigma)^{1/2}} \exp\left(-\frac{1}{2}(x - \mu)^T \Sigma^{-1}(x - \mu)\right) \quad (8)$$

HIP-NAc 2D-PDF of LFP signals are shown in Fig. 5.A. The 2D Gaussian PDF properties (Covariance and Mean) were compared, and the results show that the covariance of the food treatment group had increased from the pre- to post-conditioning phase (one-sided t-test between pre-and post-conditioning, $P < 0.05$).

To further investigate the HIP-NAc activity changes between pre-and post-conditioning phases, KLD of 2D Gaussian PDF was calculated [15]:

$$KLD(PDF_1 \parallel PDF_2) = \frac{1}{2} \left(\log \frac{\det \Sigma_2}{\det \Sigma_1} - n + \text{tr}(\Sigma_2^{-1} \Sigma_1) + (\mu_2 - \mu_1)^T \Sigma_2^{-1} (\mu_2 - \mu_1) \right) \quad (9)$$

Where 1 and 2 refer to pre-and post-conditioning, respectively.

2D-HIP-NAC KLD was calculated and compared across all treatment groups to classify treatment groups. Results show that the food treatment group had the higher HIP-NAC KLD, followed by morphine (one-way ANOVA test with post-hoc Tukey test, $P < 0.01$), and lastly, saline groups (one-way ANOVA test with post-hoc Tukey test, $P < 0.05$). Also, results show that the morphine treatment group had a higher HIP-NAC KLD than the saline treatment group (one-way ANOVA test with post-hoc Tukey test, $P < 0.01$) (Fig. 5.B). This step-wise rise enabled us to set a 2D HIP-NAC threshold, to classify subjects with 100% accuracy into the food treatment group ($0.3050 < \text{Food-threshold}$), morphine ($0.1341 < \text{Morphine-threshold} < 0.305$), and saline group ($\text{Saline-threshold} < 0.1341$).

4.5. Symmetrized dot pattern analysis (SDP)

This part used the symmetrized dot pattern technique for real-time classification and validation of recording LFP signals from deep brain regions.

The SDP method is used to visualize changes in the amplitude of time-series data that can be quickly interpreted and transform the time waveform into a scatter plot space. SDP visualizes data based on plotting each data point with bilateral mirror symmetry, having a specific six-fold symmetry shape. The technique allows rapid detection of minor changes since symmetry is a visual property quickly and efficiently detected by human perception; therefore, minor changes in input signals will be noted. SDP is defined as (10).

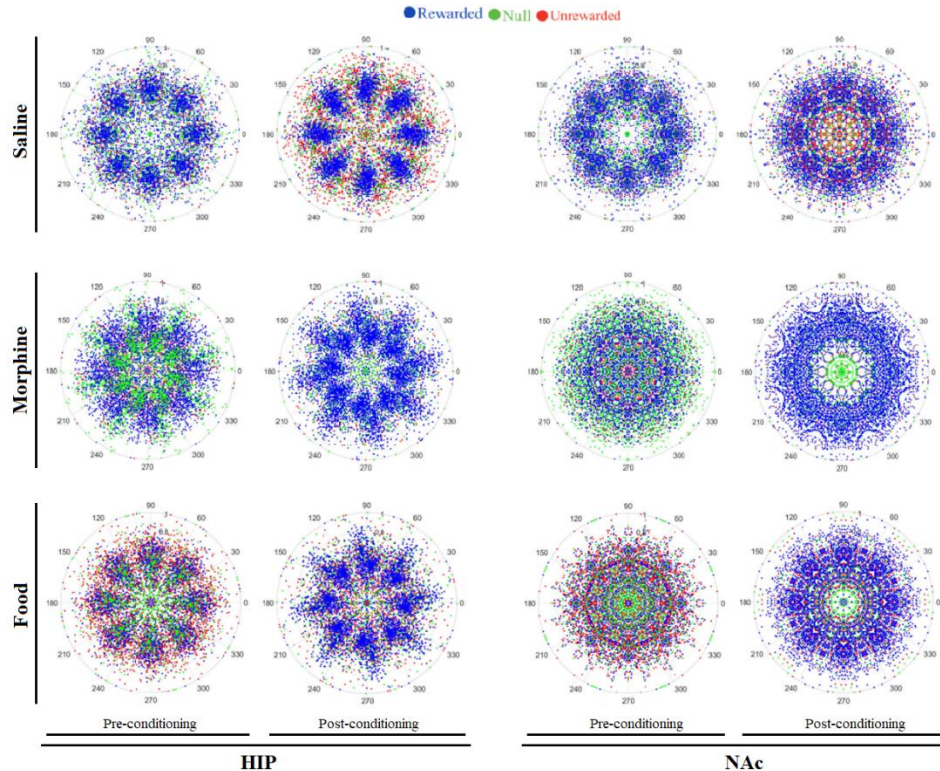


Fig. 6. Symmetrized dot pattern (SDP) visualization. Top panel: saline, middle panel: morphine, and bottom panel: food treatment groups; left panel: HIP, and right panel NAc recording sites; first and third columns: Pre-conditioning phase, second and

fourth columns: post-conditioning phase; blue dots: rewarded, green dots: Null, and red dots: unrewarded compartments. Results show that HIP is often formed a vane pattern, whilst NAc is rather polygonal with a polygonal pattern.

$$\begin{aligned}
 A(i) &= \frac{X(i)-X_{min}}{X_{max}-X_{min}} \\
 \theta(i) &= \theta + \frac{X(i+L)-X_{min}}{X_{max}-X_{min}} \zeta \\
 \Phi(i) &= \theta - \frac{X(i+L)-X_{min}}{X_{max}-X_{min}} \zeta
 \end{aligned} \tag{10}$$

Where X is the input signal, θ is the repetition or symmetry angle, L is a delay, ζ is the increase in the drawing angle, $A(i)$ are SDP radii, $\theta(i)$ is the angle of a dot in SDP, $\Phi(i)$ is the negative angle of a dot in SDP, and i is the number of selected points in signal ($i = t/\Delta t$) with Δt is the sampling rate. Experimentally, the parameters were selected as $L = 1, \theta = 45$, and $\zeta = 90$ [41].

Rapid plotting in SDP allows us to visualize the signals in real-time with many applications. For instance, this can be used to validate the placement of the LFP micro-electrodes for a specific region during a live experiment when an animal was performing the CPP as a behavioral task.

Interestingly SDP results of sample data of HIP (Fig.6, left panel) represent a pattern distinct from NAc visually, it can be seen that HIP is often formed a vane pattern, whilst NAc is rather polygonal with a polygonal pattern (Fig.6, right panel).

5. Conclusion

This study aimed to clean, validate, and classify LFP recorded data in the time-domain to investigate the activity of HIP, NAc, and connectivity of these two major regions of the reward circuit in response to morphine and food as a drug and natural reward, respectively.

The following methods were used for data validation:

- 1- Chaotic tests: Hurst and Lyapunov tests.
- 2- Non-chaotic test: Autocorrelation

Various basic and advanced time-domain methods have been successfully used to classify the data; however, some basic methods such as mean, skewness, and kurtosis have been unsuccessful. The following methods presented significant results:

- 1- HIP-NAc correlation: to classify the food group from other treatment groups (morphine and saline groups).
- 2- Difference of data PDFs:
 - 2-1- HIP\Nac 1D PDF:
 - 2-1-1- KLD test: to classify treatment groups (morphine, food, and saline groups).
 - 2-1-2- PDF's variance: to classify conditioning phases (pre- and post-conditioning phases).
 - 2-2- HIP-NAc 2D PDF:
 - 2-2-1- HIP-NAc PDSs covariance: to classify the Food group from other treatment groups (morphine and saline groups).
 - 2-2-2- KLD test: to classify treatment groups (morphine, food, and saline groups).
- 3- SDP: to classify recording sites (HIP and NAc).

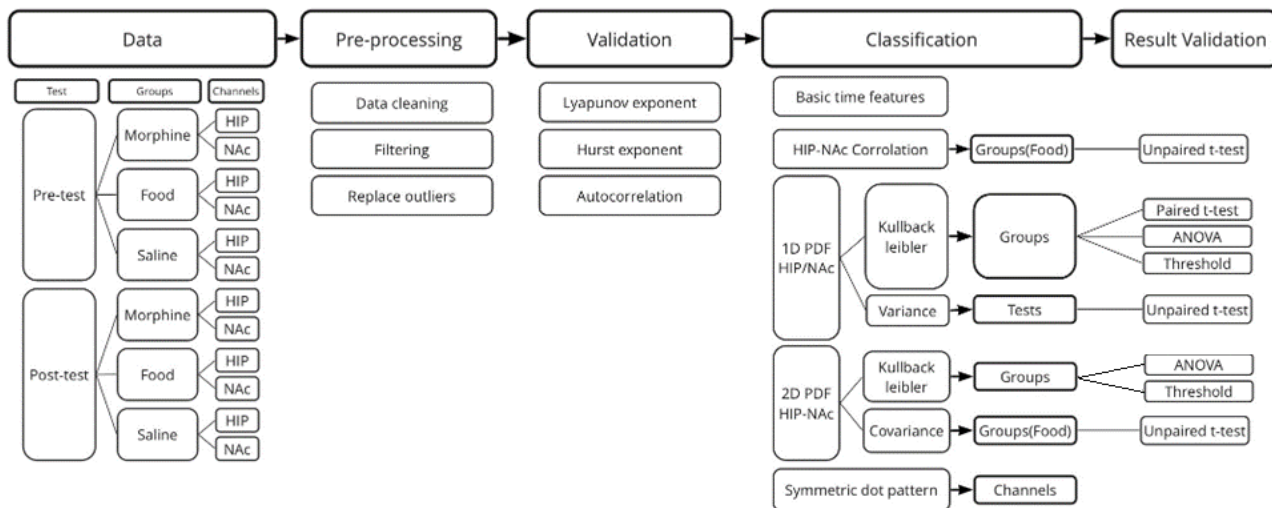


Fig. 7. The steps of classification

By using approaches in the current study (Fig7), LFP signals were classified into a source of reward (natural (food) vs. drug (morphine) vs. saline), as well as from the source of the signal (HIP vs. NAc) and conditioning phases (pre vs. post) with 100% accuracy. Our method provides a computationally light and fast, real-time signal analysis approach that can be implemented in the laboratory and in clinical settings to provide meaningful insights into deep brain activity, especially when investigating neurobehavioral neural circuits, such as addiction.

References

- [1] P. A. Adeniyi, A. Shrestha, and O. M. Ogundele, "Distribution of VTA glutamate and dopamine terminals, and their significance in CA1 neural network activity," *Neuroscience*, vol. 446, pp. 171-198, 2020.
- [2] A. S. Al-Fahoum, and A. A. Al-Fraihat, "Methods of EEG signal features extraction using linear analysis in frequency and time-frequency domains," *International Scholarly Research Notices*, vol. 2014, 2014.
- [3] J. Alvarez-Ramirez, and R. Escarela-Perez, "Time-dependent correlations in electricity markets," *Energy Economics*, vol. 32, no. 2, pp. 269-277, 2010.
- [4] P. P. Angelov, X. Gu, and J. C. Principe, "A generalized methodology for data analysis," *IEEE transactions on cybernetics*, vol. 48, no. 10, pp. 2981-2993, 2017.
- [5] P. Borgnat, P. Flandrin, P. Honeine *et al.*, "Testing stationarity with surrogates: A time-frequency approach," *IEEE Transactions on Signal Processing*, vol. 58, no. 7, pp. 3459-3470, 2010.
- [6] S. M. Bruijn, D. J. Bregman, O. G. Meijer *et al.*, "Maximum Lyapunov exponents as predictors of global gait stability: a modelling approach," *Medical engineering & physics*, vol. 34, no. 4, pp. 428-436, 2012.
- [7] J. J. Buccafusco, "Methods of behavior analysis in neuroscience," 2000.
- [8] Y. Chen, M. Ding, and J. S. Kelso, "Long memory processes (1/f α type) in human coordination," *Physical Review Letters*, vol. 79, no. 22, pp. 4501, 1997.
- [9] L. Cohen, *Time-frequency analysis*: Prentice hall New Jersey, 1995.
- [10] G. J. Dolecek, "MATLAB-based program for teaching autocorrelation function and noise concepts," *IEEE Transactions on Education*, vol. 55, no. 3, pp. 349-356, 2011.
- [11] A. F. Gill, S. A. Fatima, A. Nawaz *et al.*, "Time domain analysis of EEG signals for detection of epileptic seizure." pp. 32-35.
- [12] M. S. Granero, J. T. Segovia, and J. G. Pérez, "Some comments on Hurst exponent and the long memory processes on capital markets," *Physica A: Statistical Mechanics and its applications*, vol. 387, no. 22, pp. 5543-5551, 2008.
- [13] V. K. Harpale, and V. K. Bairagi, "Time and frequency domain analysis of EEG signals for seizure detection: A review." pp. 1-6.
- [14] D. Hernández, L. Trujillo, O. Villanueva *et al.*, "Detecting epilepsy in EEG signals using time, frequency and time-frequency domain features," *Computer science and engineering—theory and applications*, pp. 167-182: Springer, 2018.
- [15] J. R. Hershey, and P. A. Olsen, "Approximating the Kullback Leibler divergence between Gaussian mixture models." pp. IV-317-IV-320.
- [16] H. E. Hurst, "Long-term storage capacity of reservoirs," *Transactions of the American society of civil engineers*, vol. 116, no. 1, pp. 770-799, 1951.
- [17] S. Jamali, M. Aliyari Shoorehdeli, M. R. Daliri *et al.*, "Differential Aspects of Natural and Morphine Reward-Related Behaviors in Conditioned Place Preference Paradigm," *Basic and Clinical Neuroscience*, pp. 0-0.
- [18] S. Jamali, S. Zarrabian, and A. Haghparast, "Similar role of mPFC orexin-1 receptors in the acquisition and expression of morphine-and food-induced conditioned place preference in male rats," *Neuropharmacology*, vol. 198, pp. 108764, 2021.
- [19] S. Ji, Z. Zhang, S. Ying *et al.*, "Kullback-leibler divergence metric learning," *IEEE Transactions on Cybernetics*, 2020.
- [20] H. Kantz, "A robust method to estimate the maximal Lyapunov exponent of a time series," *Physics letters A*, vol. 185, no. 1, pp. 77-87, 1994.
- [21] M. Karanasos, Z. Psaradakis, and M. Sola, "On the Autocorrelation Properties of Long-Memory GARCH Processes," *Journal of Time Series Analysis*, vol. 25, no. 2, pp. 265-282, 2004.
- [22] S.-J. Leigh, and M. J. Morris, "The role of reward circuitry and food addiction in the obesity epidemic: An update," *Biological psychology*, vol. 131, pp. 31-42, 2018.
- [23] M. Lew-Starowicz, K. Lewczuk, I. Nowakowska *et al.*, "Compulsive sexual behavior and dysregulation of emotion," *Sexual medicine reviews*, vol. 8, no. 2, pp. 191-205, 2020.
- [24] T. W. Lo, J. W. Yeung, and C. H. Tam, "Substance abuse and public health: A multilevel perspective and multiple responses," 7, Multidisciplinary Digital Publishing Institute, 2020, p. 2610.
- [25] D. J. MacKay, and D. J. Mac Kay, *Information theory, inference and learning algorithms*: Cambridge university press, 2003.
- [26] G. Martin, S. H. Ahmed, T. Blank *et al.*, "Chronic morphine treatment alters NMDA receptor-mediated synaptic transmission in the nucleus accumbens," *Journal of Neuroscience*, vol. 19, no. 20, pp. 9081-9089, 1999.

- [27] R. Mozafari, S. Jamali, M. Pourhamzeh *et al.*, "The blockade of D1-and D2-like dopamine receptors within the dentate gyrus attenuates food deprivation stress-induced reinstatement of morphine-extinguished conditioned place preference in rats," *Pharmacology Biochemistry and Behavior*, vol. 196, pp. 172967, 2020.
- [28] I. J. Myung, "Tutorial on maximum likelihood estimation," *Journal of mathematical Psychology*, vol. 47, no. 1, pp. 90-100, 2003.
- [29] M. Nazarathy, W. V. Sorin, D. M. Baney *et al.*, "Spectral analysis of optical mixing measurements," *Journal of Lightwave technology*, vol. 7, no. 7, pp. 1083-1096, 1989.
- [30] F. Nazari-Serenjeh, S. Jamali, L. Rezaee *et al.*, "D1-but not D2-like dopamine receptor antagonist in the CA1 region of the hippocampus reduced stress-induced reinstatement in extinguished morphine-conditioning place preference in the food-deprived rats," *Behavioural Pharmacology*, vol. 31, no. 2-3, pp. 196-206, 2020.
- [31] F. Nazarimehr, S. Jafari, S. M. R. Hashemi Golpayegani *et al.*, "Can Lyapunov exponent predict critical transitions in biological systems?," *Nonlinear Dynamics*, vol. 88, no. 2, pp. 1493-1500, 2017.
- [32] C. M. Olsen, "Natural rewards, neuroplasticity, and non-drug addictions," *Neuropharmacology*, vol. 61, no. 7, pp. 1109-1122, 2011.
- [33] J. K. Patel, and C. B. Read, *Handbook of the normal distribution*: CRC Press, 1996.
- [34] B. Qian, and K. Rasheed, "Hurst exponent and financial market predictability." pp. 203-209.
- [35] Z. Rached, F. Alajaji, and L. L. Campbell, "The Kullback-Leibler divergence rate between Markov sources," *IEEE Transactions on Information Theory*, vol. 50, no. 5, pp. 917-921, 2004.
- [36] S. Riaz, A. Schumacher, S. Sivagurunathan *et al.*, "Ventral, but not dorsal, hippocampus inactivation impairs reward memory expression and retrieval in contexts defined by proximal cues," *Hippocampus*, vol. 27, no. 7, pp. 822-836, 2017.
- [37] P. J. Rogers, "Food and drug addictions: Similarities and differences," *Pharmacology Biochemistry and Behavior*, vol. 153, pp. 182-190, 2017.
- [38] C. Rudin, "Stop explaining black box machine learning models for high stakes decisions and use interpretable models instead. *Nat Mach Intell*. 2019; 1: 206–15."
- [39] L. L. Scharf, and C. Demeure, *Statistical signal processing: detection, estimation, and time series analysis*: Prentice Hall, 1991.
- [40] G. Shevlyakov, and M. Kan, "Stream data preprocessing: Outlier detection based on the chebyshev inequality with applications." pp. 402-407.
- [41] K. Shibata, A. Takahashi, and T. Shirai, "Fault diagnosis of rotating machinery through visualisation of sound signals," *Mechanical Systems and Signal Processing*, vol. 14, no. 2, pp. 229-241, 2000.
- [42] G. D. Stuber, D. R. Sparta, A. M. Stamatakis *et al.*, "Excitatory transmission from the amygdala to nucleus accumbens facilitates reward seeking," *Nature*, vol. 475, no. 7356, pp. 377-380, 2011.
- [43] Y. L. Tong, *The multivariate normal distribution*: Springer Science & Business Media, 2012.
- [44] W. Van Drongelen, *Signal processing for neuroscientists*: Academic press, 2018.
- [45] N. D. Volkow, M. Michaelides, and R. Baler, "The neuroscience of drug reward and addiction," *Physiological reviews*, vol. 99, no. 4, pp. 2115-2140, 2019.
- [46] A. Vulpiani, F. Cecconi, and M. Cencini, *Chaos: from simple models to complex systems*: World Scientific, 2009.
- [47] T. Weiland, "Time domain electromagnetic field computation with finite difference methods," *International Journal of Numerical Modelling: Electronic Networks, Devices and Fields*, vol. 9, no. 4, pp. 295-319, 1996.
- [48] C. Ziehmann, L. A. Smith, and J. Kurths, "Localized Lyapunov exponents and the prediction of predictability," *Physics Letters A*, vol. 271, no. 4, pp. 237-251, 2000.